The influence of warm forming in natural aging and springback of Al-Mg-Si alloys

Vasco Simões, Hervé Laurent, Marta Oliveira, Luís Menezes

The influence of warm forming in natural aging and springback of Al-Mg-Si alloys

Vasco Simões [a,b,*], Hervé Laurent [a], Marta Oliveira [b], Luís Menezes [b]

[a] Univ. Bretagne Sud, FRE CNRS 3744, IRDL, F-56100 Lorient, France.

[b] CEMMPRE, Department of Mechanical Engineering, University of Coimbra, Polo II, Rua Luís Reis Santos, Pinhal de Marrocos, 3030-788 Coimbra, Portugal

* Corresponding author: vasco.simoes@uc.pt (+351 912536771)

Abstract

Warm forming is a very interesting solution to improve formability and reduce springback. Natural aging is an open issue for heat treatable aluminum alloys, since it causes variability in sheet metal forming operations, namely in the parts shape, as well as in-service behavior. Therefore, this work aims to study the contribution of warm forming to minimize the variability caused by natural aging and reduce the springback in sheet metal forming operations. The thermo-mechanical behavior of two Al-Mg-Si alloys, EN AW 6016-T4 and EN AW 6061-T6, is studied in function of temperature (from 22 to 300°C) using uniaxial tensile tests, cylindrical cup tests and split ring (springback) tests. Moreover, for the EN AW 6016-T4, the study was also performed in function of the storage time (from 1 to 18 months). At 22°C, the increase of the storage time leads to a clear increase of the yield stress and of the work hardening and, consequently, of the springback. Warm forming at temperatures between 200 and 250°C, using a short exposure time, reduces the yield stress and the work hardening and, consequently, springback for both alloys. Moreover, the effect of natural aging is minimized. Thus, warm conditions can be used as an effective solution to minimize the variability caused by the natural aging and reduce the springback in forming operations of heat treatable aluminum alloys.

Keywords: Al-Mg-Si; Natural Aging; Warm Forming; Springback

1 Introduction

The increasing demand for aluminum alloys in the automotive sector is linked with their good strength-to-weight ratio, leading to lower weight and consequent emissions reduction during vehicles life cycle [1]. However, when compared with conventional steels, the aluminum alloys present lower formability and higher springback. Warm forming has been used as a solution to improve formability of non-heat and heat treatable aluminum alloys [2, 3]. Moreover, warm forming has been also reported as a solution to reduce springback of non-heat treatable alloys [4, 5], but the influence of warm forming in springback of heat treatable alloys has not been previously studied.

Heat treatable aluminum alloys have the advantage of changing their ductility and strength in function of heat treatment conditions [6]. Ductility is required for sheet metal forming operations while strength is required for in-service behavior. The heat treatment consists of solution heat treatment (SHT) followed by the rapid quenching until room temperature (RT) (as-quenched state) and, subsequent precipitation hardening. The SHT dissolves the alloying elements in the aluminum matrix, while the rapid quenching to RT creates a metastable equilibrium due to the supersaturation of the alloying elements at RT. This metastable equilibrium is the driving force for precipitation (aging). In the present study, the heat treatable Al-Mg-Si alloys (6xxx series) were selected since they are highly demanded by the automotive industry. In these alloys, precipitation occurs by diffusion mainly assisted by “quenched-in vacancies”, since Mg and Si are substitutional elements in the aluminum matrix. Natural aging refers to the precipitation that occurs at RT during storage time. Artificial aging refers to a subsequent heating stage, at a temperature range between 170 and 200 °C, which is required to obtain the maximal strength.

The natural aging is a spontaneous phenomenon that depends of the storage time at RT. For example, in the stretch forming of an aircraft skin, Suri et al. [7] concluded that natural aging can lead to 23% of strain variation and 9% of thickness variation. In fact, natural aging increases the yield stress and of the work hardening [8, 9], which are the most influential parameters in springback and thinning variability, respectively [10]. Moreover, in 7xxx series the orthotropic behavior changes from in-plane isotropic behavior, in the as-quenched state, to in-plane anisotropy, during the first 15 min of natural aging [9]. However, after this abrupt change, the

degree of anisotropy appears to remain constant. Regarding the formability, Prillhofer et al. [11] studied four different Al-Mg-Si alloys concluding that the forming limit curves and the bendability slightly decrease due to natural aging. Thus, sheet metal forming of heat treatable alloys poses an additional difficulty connected with the variability of their mechanical behavior due to the natural aging, which can lead to the lack of dimensional accuracy in the production lines [7, 11].

Some solutions were proposed in the literature aiming to avoid the natural aging after as-quenched state, which contributes to decrease the peak strength obtained after artificial aging. These solutions are: interrupted quenching [12], pre-aging [12, 13], pre-strain [13, 14], and pre-strain followed by pre-aging [13]. These methods promote the formation of Mg-Si clusters, which reduce the supersaturation of alloying elements and the number of “quenched-in vacancies” [12]. However, none of these methods can definitely suppress the natural aging. In fact, they can only stabilize natural aging during reduced time spans (up to few days), which is not enough for industrial practice, where the time span between as-quenched state and sheet metal forming can be delayed from several weeks up to a few months [14]. Thus, Suri et al. [7] proposed the standardization of the storage time to control the material properties at the forming instant. Recently, Werinos et al. [15] shown that the addition of Sn in the composition of Al-Mg-Si alloys traps the quenched-in vacancies essential for diffusion and allows the temporary suppression of natural aging, up to a maximum of 6 months.

The study of Al-Mg-Si alloys with different compositions using differential scanning calorimetry analysis shows that the natural aging clusters dissolve in a temperature range between 200 and 250 °C [13]. Similar conclusions were reported Pogatscher et al. [16] by hardness data analysis. Additionally, the temperature increase contributes to minimizing the interactions between natural aging clusters and dislocations, improving the dislocation motion. Both mechanisms, the dissolution of natural aging clusters and the improvement of the dislocation motion, are expected to minimize the natural aging effect at the warm forming condition, for this temperature range. Nevertheless, for Al-Mg-Si alloys, the warm forming above 200°C can be counterproductive for the post forming properties, since it can lead to the decrease of the strength required for in-service behavior [17]. In fact, warm forming of heat treatable alloys requires an improved knowledge of the interaction between precipitation kinetics and temperature, exposure time and degree of deformation [18]. According to Ghosh et al. [19] and Kumar et al. [18], a reduced exposure time

is an effective means to minimize the occurrence of counterproductive precipitation during warm forming processes. In fact, the warm forming of an 7xxx-high strength aluminum at 170°C with just one or two minutes of process time has almost no impact on its strength [20]. Thus, in order to minimize the heat treatment change, in the present work the total exposure time (heating and forming time) of the material at warm forming temperature was always inferior to 2 min.

In this context, the present work aims to improve knowledge concerning the influence of warm forming conditions on the springback behavior of two Al-Mg-Si alloys. The influence of natural aging in their mechanical behavior is analyzed, particularly the potential of using warm forming conditions to reduce variability in sheet metal forming operations, namely in springback. The identification of natural aging precipitates is extremely difficult due to its nanometer size, particularly for Al-Mg-Si alloys [21]. Thus, the influence of natural aging was studied following a macroscopic approach, using uniaxial tensile tests, cylindrical cup tests and the split ring tests.

2 Materials

The two alloys selected for this study are the EN AW 6016-T4 and the EN AW 6061-T6, which are commonly used for skin applications and for structural components in the automotive industry, respectively. The designation T4 indicates solution heat treated and naturally aged to a substantially stable condition, while the designation T6 indicates solution heat treated followed by artificial aging. The mechanical properties of both alloys and the thickness are presented in Table 1. The terms and definitions used throughout this work are according to ISO 6892-1:2009 [22] (i.e. R_m tensile strength; $R_{p0.2}$ proof strength at 0.2% of the extensometer gauge length; A_g percentage of non-proportional elongation at maximum force). Table 2 presents the mass fraction of the main alloying elements (in percent composition by mass, wt.%) for each of the alloys under study.

The differences in the mechanical behavior of both alloys are mainly linked with the heat treatments, since the T4 heat treatment is used to attain higher ductility, while the T6 heat treatment is used to attain higher the strength. In fact, a previous study shows that both alloys present similar thermo-mechanical behavior for the same heat treatment condition [23]. Since warm conditions can promote a change of the heat treatment conditions, using alloys with different heat treatments provides a reference to evaluate the occurrence of microstructural changes.

Finally, the study of both alloys also provides a complete understanding of the springback behavior of heat treatable alloys under warm forming conditions.

The EN AW 6016-T4 alloy was provided by Constellium and the date of the SHT is known; therefore, its storage time at RT is counted after the date of the SHT. The EN AW 6061-T6 alloy was acquired in the retail market and the date of SHT and T6 heat treatment is unknown; therefore, its storage time at RT is counted after its reception in the laboratory. Prillhofer et al. [11] analyzed the natural aging of four Al-Mg-Si alloys in T4 and T6 condition, concluding that natural aging is susceptible to occurs for both heat treatments. Therefore, the influence of natural aging in the thermo-mechanical behavior during the study period is evaluated for both alloys.

	$R_{p0.2}$	R_m	A_g	Thickness
EN AW 6016-T4	88 MPa	198 MPa	24.6 %	1.05 mm
EN AW 6061-T6	≈275 MPa	≈310 MPa	≈10 %	0.98 mm

Table 1 – Mechanical properties of the EN AW 6016-T4 alloy at 4 days of maturation (supplier results) and of the EN AW 6061-T6 alloy [24]. The thickness presented corresponds to the average value obtained with fifty measurements.

	Si	Mg	Cu	Fe	Mn	Mg+Si+Cu	Mg/Si
EN AW 6016-T4	0.91	0.41	0.10	0.255	0.17	1.42	0.45
EN AW 6061-T6	0.4-0.8	0.8-1.2	0.15-0.4	<0.70	<0.40	1.35-2.4	1.0-3.0

Table 2 – Chemical composition, in percent composition by mass (wt.%), of the EN AW 6016-T4 (supplier results) and the EN AW 6061-T6 [25] alloys.

3 Thermo-mechanical characterization

3.1 Experimental procedure

The thermo-mechanical behavior was evaluated performing uniaxial tensile tests in a Gleeble 3500 device, being the strain fields acquired using digital image correlation (system ARAMIS 4M – GOM) and the temperature with type K thermocouples welded on the specimen surface. A detailed description of the test procedure adopted is presented in [26]. The tensile tests were performed at RT (≈22), 100, 150, 200 and 300°C, considering an imposed initial strain rate of ≈ $2x10^{-3}s^{-1}$. The in-plane anisotropic behavior and the natural aging effect were studied from RT up to 200°C, using specimens cut along three different directions in the sheet plane: 0, 45 and 90°,

with the rolling direction (RD). The heating time is fixed to 20 seconds in order to minimize microstructural modifications while assuring that the required temperature in the specimen center is achieved. A minimum of two tensile tests was performed for each test condition. The reproducibility was confirmed by the average scatter of the true stress, which was less than ±1MPa for the same true strain value. Therefore, only one representative test is presented for each condition. The tensile test results are presented as true stress – true strain plotted until the maximum load.

3.2 Results analysis and discussion

3.2.1 The hardening behavior

The true stress – true strain curves are presented in Figure 1 a) and b) for the EN AW 6016-T4 and EN AW 6061-T6 alloys, respectively. The results show that for the EN AW 6016-T4 alloy a noteworthy variation of the mechanical properties due to the storage time is observed, while it is negligible for the EN AW 6061-T6 alloy. The dependence of the material behavior to temperature is similar for both alloys, i.e. as the temperature increases the flow stress decreases resulting in lower values of $R_{p0.2}$ and R_m, in agreement with [23, 27]. However, for the same temperature, the mechanical behavior of both alloys is distinct. In fact, the EN AW 6061-T6 alloy presents always a higher strength and a lower true strain value than the EN AW 6016-T4 alloy.

Concerning the EN AW 6016-T4 alloy (see Figure 1 a)), the natural aging leads to an increase of the material strength, introducing also a variation of the work hardening behavior. Comparing the stress-strain curves at 1 and 7 months of natural aging, the difference in stress values for the same strain value reduces with the increase of temperature. At RT, the increase of storage time leads to the increase of the $R_{p0.2}$ value and a slight increase of the work hardening rate. At 200 °C the natural aging effect is still observed by the increase of the $R_{p0.2}$ value, but it leads to a decrease of the work hardening rate. In fact, at 200 °C for strain values higher than 10%, the stress-strain curves of 1 and 7 months aged specimens present a similar hardening behavior with approximately the same R_m value. This may be linked with the dissolution of Mg-Si co-clusters that occurs for the temperature range from 200 °C to 250 °C, as reported in previous studies [13, 16]. At 200 ºC, the time necessary to attain a strain of 10% is 40 seconds. Taking into account

the heating time of 20 seconds, the analysis of the stress-strain curves indicates that the time to dissolve natural aging Mg-Si co-clusters is about 60 seconds.

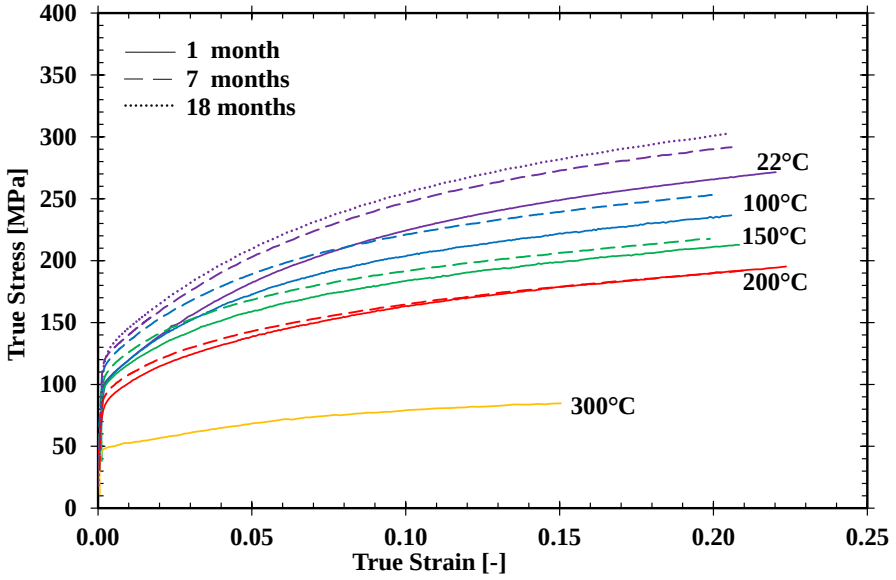

a) EN AW 6016-T4

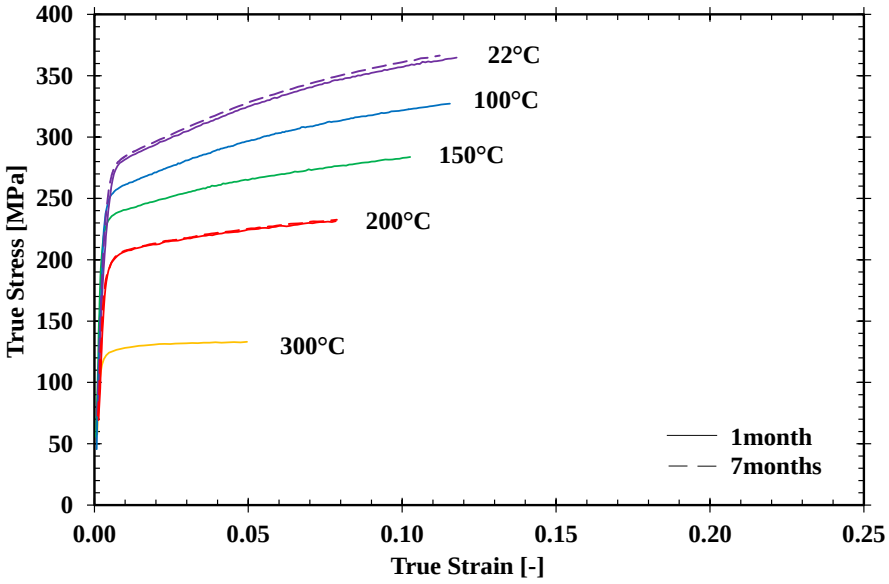

b) EN AW 6061-T6

Figure 1 – Influence of the natural aging on the true stress – true strain curves obtained from uniaxial tensile tests performed at different temperatures, for specimens oriented along the RD at 1 and 7 months of storage time. The 1 month aged material is shown by the solid line and the 7 months by the dashed line.

The percentage of total elongation as a function of the temperature is presented in Figure 2. The total elongation is the sum of the elastic and the plastic one [22], and its analysis is performed at

maximum force (A_{gt}) and at fracture (A_t). The A_t values corresponds to the first strain value (after the A_{gt}) with a stress value (σ_{At}) that complies with the requirement: $\sigma_{At} \approx 0.9R_m$. The values reported in Figure 2 correspond to the average of the several uniaxial tensile tests performed, including all the in-plane orientations (0, 45, 90°) to the RD. Thus, the error bars present the global minimum and maximum values obtained, with the black color associated to the 7 months tests.

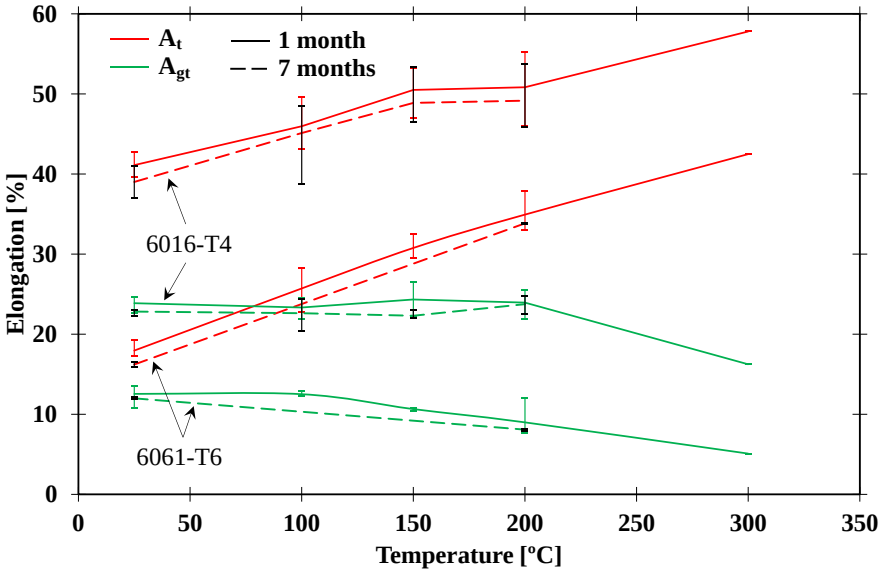

Figure 2 – Evolution of the percentage of total elongation at maximum force (A_{gt}) and at fracture (A_t) in function of temperature The error bars show the minimum and maximum values obtained for all the tests performed (0, 45, 90° to the RD), with the black color associated to the 7 months tests.

Figure 2 shows that, for both alloys and whatever the temperature, the 7 months aged specimens presents a slightly lower elongation value at A_{gt} and A_t than the 1 month ones. Concerning the temperature influence between RT and 200 °C, the A_t value increases with temperature, presenting an increase greater than 10%, for both alloys. On the other hand, the A_{gt} value remains almost constant, for the EN AW 6016-T4, or even decreases, for the EN AW 6061-T6 alloy. Moreover, in a temperature range from 200 to 300 °C, the A_{gt} values present an abrupt decrease for both alloys, while the A_t values keeps increasing. It denotes that, the ductility enhancement at elevated temperatures is achieved primarily by the post-uniform elongation (i.e. the diffuse necking, the strain difference between the on-set of necking, A_{gt}, and A_t) which becomes dominant at elevated temperatures [3]. This behavior is similar to the one previously reported in [28, 29] but in that case for Al-Mg alloys, where it was stated that this overall increase of ductility

should be advantageous, since the industrial criterion for a successful sheet metal forming part only requires neither a severe thinning nor a crack in the part.

3.2.2 Strength evolution as a function of the storage time for the EN AW 6016-T4 alloy

As previously shown in Figure 1, the influence of the storage time in the variation of the material behavior is relevant only for the EN AW 6016-T4 alloy and at RT. In literature, the most reported influence of natural aging is the material strength increase in function of storage time. According to Esmaeili and Lloyd [30] and Hirth et al. [31], the material strength evolution follows a linear relationship with the logarithm of storage time, as follows:

$$R_{t_{NA}} = k\log(t_{NA}) + R_i, \quad (1)$$

where $R_{t_{NA}}$ is the yield stress, t_{NA} is the storage time, k is the natural aging kinetics parameter and R_i represents the initial yield stress of the alloy, measured after quenching and storage at RT for ≈1 h. Thus, the determination of the natural aging kinetics parameter enables the prediction of the strength increase. In the present study, k was determined equal to 19.7 considering the R_i value of 88 MPa, obtained after 4 days of natural aging (see Table 1).

The analysis of natural aging kinetics for the EN AW 6016-T4 is presented in Figure 3, considering a summary of the results collected from literature and the ones of the present study. The stress evolution is correlated with the storage time, according to Equation 1. The goal is to present a range for the yield stress evolution and better understand the natural aging kinetics. According to Equation 1, Figure 3 traduces the linear increase of the stress value in function of the logarithm of the storage time. Nonetheless, a high scatter of the yield stress values is observed for the same storage time, which disables any prediction of this value in function of the natural aging based on literature results. In accordance with previous studies [30–32], this high scatter can be related to slight differences in the chemical composition. Hirth et al. [31] and Esmaeili and Lloyd [30] showed that increasing the Si content (within standards chemical composition limits) promotes the increase of the initial yield while the natural aging kinetics remains unaltered. Nevertheless, the natural aging kinetics depends more on the Mg+Si content than on the Mg/Si ratio [32]. Moreover, Ding et al. [32] and Esmaeili and Lloyd [30] also showed that increasing the Cu content is linked with the increase of natural aging kinetics, while it also promotes a decrease of the initial yield stress. Therefore, in the present work the amount of Mg+Si+Cu was adopted as reference (see

Table 2), since alloys with a higher content of these alloying elements are more saturated, and therefore, the driving force for precipitation is higher.

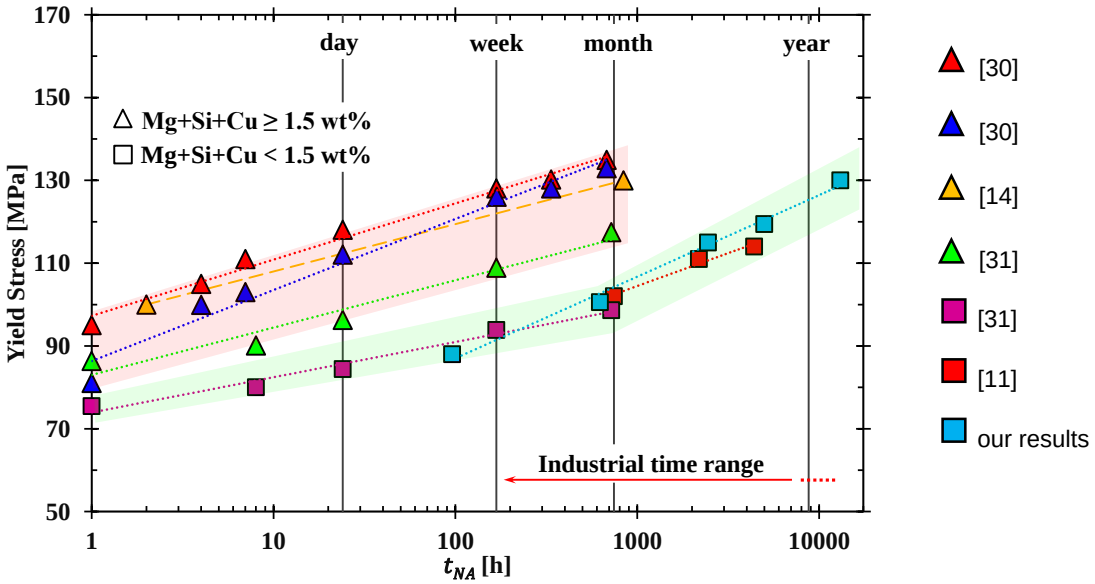

Figure 3 – The stress evolution as function of the storage time (t_{NA}) in logarithmic scale, according to Equation 1, for the EN AW 6016-T4 alloy. The results found in literature are presented with the ones of the present study in order to better understand the natural aging kinetics.

In this context, it was decided to divide the literature results presented in Figure 3 into two groups: (i) the group of alloys where Mg+Si+Cu < 1.5 [wt.%] (in green) and (ii) the group where Mg+Si+Cu ≥ 1.5 [wt.%] (in red). The alloy considered in this study presents an amount of Mg+Si+Cu = 1.42 [wt.%] (see Table 2) and, its natural aging behavior is, in fact, similar to the other alloys located in the green region of Figure 3. However, the natural aging kinetics parameter also varies with the storage time as indicated in Figure 3 by the change of slope for the green region. In fact, recent studies reported the existence of five different natural aging stages in Al-Mg-Si alloys, each one with its own kinetics [15, 33]. Therefore, the natural aging kinetics parameter is valid only within a limited storage time range [31]. This highlights that Equation 1 is not applicable for very short or very long natural aging times, since the natural aging kinetics and magnitude of strength increase seem dependent of storage temperature, chemical composition and degree of supersaturation [15]. Therefore, it is dangerous to extrapolate the behavior predicted by Equation 1.

3.2.3 The orthotropic behavior

This section studies the in-plane anisotropic behavior of both alloys in function of temperature and storage time. Figure 4 presents the true stress – true strain curves obtained after 1 month of storage time for the three in-plane directions, 0, 45 and 90° to the RD, in a temperature range between RT and 200 °C, for both alloys. Globally, both alloys present a small variation of the flow stress in the sheet plane, particularly the EN AW 6061-T6 alloy. The EN AW 6016-T4 alloy shows a slightly higher flow stress at the RD, whatever the temperature. Although not shown here, the tensile tests performed for the EN AW 6016-T4 alloy after 7 months of storage also reveal a negligible anisotropy of the flow stress, i.e. the trend between the different directions remains the same.

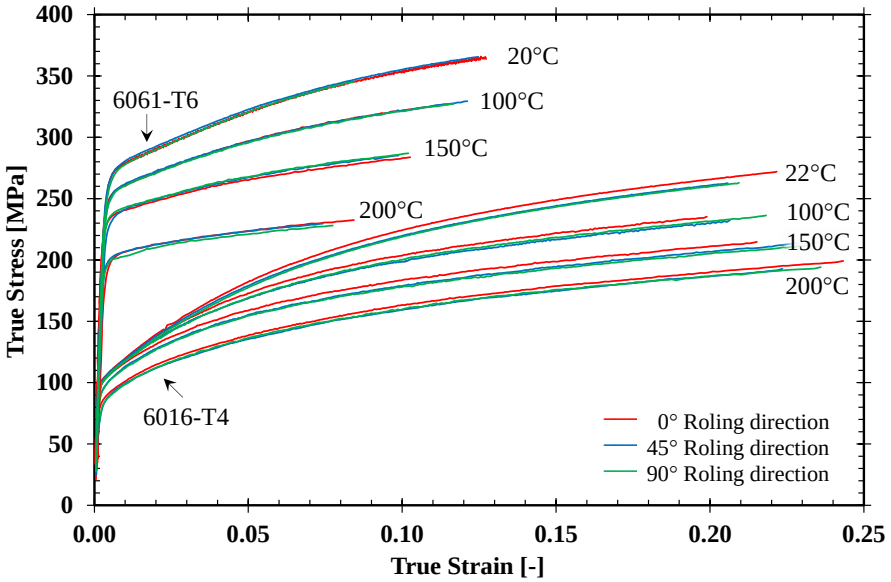

Figure 4 – Influence of temperature and orientation to RD on the true stress – strain curves, performed from RT to 200 °C; at 0, 45, 90° to RD. Tests performed at 1 month of storage time.

The anisotropy coefficient (r_α, α: angle with RD) represents the ratio between the plastic strain in the width direction (ε_{yy}^p) and the plastic strain in the thickness direction (ε_{zz}^p). During the uniaxial tensile test, the local total strain along the length (ε_{xx}) and the width (ε_{yy}) directions were acquired by the ARAMIS-GOM system. The plastic strain is obtained from the total strain by removing the elastic component. The thickness strain is determined based on the volume conservation assumption, i.e. $\varepsilon_{zz}^p = -\left(\varepsilon_{xx}^p + \varepsilon_{yy}^p\right)$. The r_α were determined based on the linear fit between ε_{yy}^p

and ε_{zz}^{p}, considering the test results up to the R_m point. The planar anisotropy coefficient (Δr) is calculated by: $\Delta r = (r_0 - 2r_{45} + r_{90})/2$, and the normal anisotropy coefficient (r_n), by: $r_n = (r_0 + 2r_{45} + r_{90})/4$.

The anisotropy coefficients are summarized in Table 3. Globally, their variations with temperature and natural aging are subtle. For the EN AW 6016-T4 alloy, the r_α value is always lower at 45° and higher at RD, whatever the temperature under analysis; while the r_n value slightly increases and the Δr value slightly decreases with the increase of the temperature, as previously observed [19]. Moreover, although the trend for the r_α values remains unaltered throughout the natural aging, natural aging contributes to the increase of the Δr value, whatever the temperature. A similar anisotropic behavior at RT was observed for the EN AW 7075 alloy for a prolonged natural aging [9]. For the EN AW 6061-T6 alloy, the r_α value is lower at 90° and higher at RD, whatever the temperature under analysis; while the r_n value remains constant and the Δr value slightly decreases with the temperature increase. The increase of the r_n value with the increase of temperature represents an advantage, since it contributes to reduce the thinning problems during sheet metal forming. The reduction of the Δr value indicates a trend to a more transverse isotropic behavior promoted by the temperature increase, which is also positive in sheet metal forming. In brief, the degree of anisotropy remains constant, independently of the storage time, temperature or their combined influence.

		EN AW 6016-T4					EN AW 6061-T6				
		r_0	r_{45}	r_{90}	r_n	Δr	r_0	r_{45}	r_{90}	r_n	Δr
1 month	RT	0.672	0.585	0.617	0.615	0.030	0.712	0.565	0.548	0.587	0.022
	100	0.665	0.594	0.634	0.622	0.028	0.723	0.572	0.562	0.607	0.035
	150	0.668	0.594	0.639	0.623	0.030	0.656	0.579	0.533	0.587	0.008
	200	0.676	0.611	0.626	0.631	0.020	0.682	0.597	0.548	0.606	0.009
	300	0.675	–	–	–	–	0.697	–	–	–	–
7 months	RT	0.664	0.577	0.642	0.615	0.038	0.677	–	–	–	–
	100	0.683	0.587	0.649	0.627	0.040	–	–	–	–	–
	150	0.672	0.586	0.641	0.621	0.036	–	–	–	–	–
	200	0.678	0.609	0.639	0.634	0.025	0.686	–	–	–	–

Table 3 –Average values of the anisotropy coefficients obtained for the EN AW 6016-T4 and the EN AW 6061-T6 alloys, at 0, 45, 90° to RD, normal (r_n) and planar anisotropy coefficient (Δr).

4 Warm forming of a cylindrical cup

The cylindrical cup forming and the springback evaluation allow a better understanding of the alloys thermo-mechanical behavior. Since only the EN AW 6016-T4 alloy is sensible to natural aging, the impact of warm forming was studied considering 1 and 18 months of storage time. Regarding the EN AW 6061-T6 alloy, the tests were performed only for 18 months.

4.1 Experimental procedure

The cylindrical cup benchmark tests were performed in a Zwick BUP200 machine, adapted with specific tools for warm forming. This dispositive was previously used to study the AA5754-O alloy [34, 35]. Before the forming process, a circular blank with 60 mm of diameter is cut out from the initial sheet by squaring shear in the Zwick BUP200, using a specific blade tool. To fully deep draw the cylindrical cup four tools were used: die, blank-holder, punch and ejector, as presented in Figure 5. The dimensions of the tools are also presented in Figure 5 a). All tests were performed with a standard clamping force of 6 kN and a punch speed of 1 mm/s. During each test, the punch force and displacement, the blank-holder force and the temperature were acquired in function of time. A minimum of three reproducible tests was performed for each condition under analysis. Their reproducibility was confirmed by the average scatter of the punch force, which was less than ±0.1kN for the same displacement. Therefore, only one representative test is presented for each condition.

The procedure used to fully deep draw the cylindrical cup is presented in Figure 5 b) to e). Figure 5 b) shows the tools in the initial position, with the blank-holder clamping the sheet against the die. However, in the warm forming tests it is necessary to pre-heat the tools and the blank. In this heating step, the die and the blank-holder were heated to the test desired temperature by internal electrical heating rods; while the punch was refrigerated to keep its temperature close to RT. When the die and the blank-holder attain the desired temperature, the blank (lubricated with a high-temperature aerosol grease 95cSt [36]) was positioned in the blank-holder. The blank is not heated at the same time that the tools, in order to reduce its heating time and, consequently, avoid microstructural modification induced by a prolonged heating stage. Due to the contact with the heated blank-holder, the blank (at RT) takes approximately 60 seconds to attain the blank-holder temperature. Once the blank, the die and the blank-holder are at the test temperature

(within a margin of error less than 2.5%), the blank-holder clamps the sheet against the die. Then, the punch was moved into the die's cavity (Figure 5 c)) to deform the blank to its final shape (Figure 5 d)). At the end of the drawing process the punch stops. Finally, the ejector was activated to remove the cup from the die's cavity (Figure 5 e)).

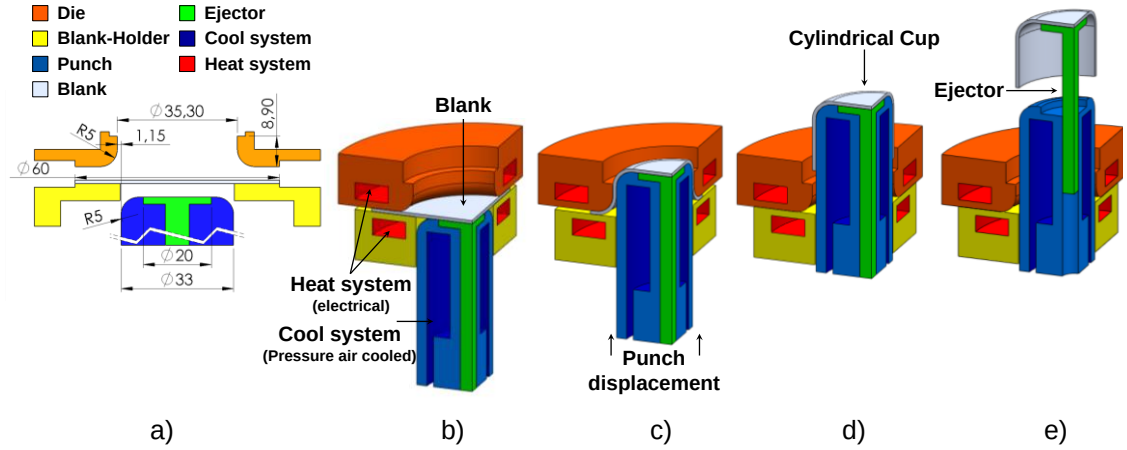

Figure 5 – Drawing of a cylindrical cup: a) Tools dimensions (in mm); b) Initial position; c) Cup drawing; d) Punch final position; and e) Ejection step.

After the forming operation, the thickness and the cup height were measured using a 3D measurement machine "*Brown & Sharpe Mfg. Co.*" model "*MicroXcel PFX-454*". The thickness measurements were performed at each 45°, from 0 to 315° to RD (see Figure 6 a)), for each drawn cup. The cup height is measured at each 5° along the cup edge (the orange points on Figure 6 a)), with the first measurement point at 0° with the RD. In order to minimize the measurement errors related with axisymmetric deviations, the thickness and the height of the cup are presented as the average of the cup vertical axis symmetries (i.e. the presented 1st quadrant from 0 to 90° to RD is an average of the 1st, 2nd, 3th and 4th quadrants). It should be mentioned that the accuracy in the thickness measurements depends on: the 3D measurement machine accuracy (±3μm), the control of the positioning of the cup on the measurement device (±15μm), and of the angular deviations to the RD direction (±5μm) [34].

Springback is analyzed using the split ring test, which according to ASTM E2492-07(2012) [37], consist on: i) cut a ring from the cup wall (trimming); ii) open the ring along the RD (split ring); and iii) measure the ring opening. An electrical discharge machining (EDM) was used to open and cut the rings, as also suggested in ASTM E2492-07(2012) [37]. The variation of the ring diameter,

before and after splitting, gives an indirect measure of the springback phenomenon and of the amount of the circumferential residual stresses present in the formed cup [5]. The ring opening was measured using a microscope to assure high measurement accuracy, and the EDM cut thickness (0.3 mm) was taken into account in the measured value.

In the present work, two modifications were made to the standard procedure. The first is related to the sequence adopted to cut the ring the from the cup: as shown in Figure 6 b), the cup was cut first along the axial direction and only afterward the rings were trimmed (see Figure 6 c)). This approach was adopted to avoid the presence of any burrs on the split ring surface, which reduce the accuracy of the ring-opening measurements. In fact, with the standard procedure ASTM E2492-07(2012) [37], during the split ring operation the internal stresses present in the ring promote a sudden rupture, leading to a burr. By performing the vertical cut first, a progressive ring opening occurs during the trimming operation. It allows a better final surface and therefore accurate measurements of the ring-opening are possible. The second modification is related to the number of rings extracted from the vertical wall, which in the present case were three, each one with 3 mm height, as shown in Figure 6 c). This procedure allows a more detailed analysis of the springback behavior, since it was previously shown that the magnitude of the ring opening is influenced by its vertical position along the cup wall [38, 39].

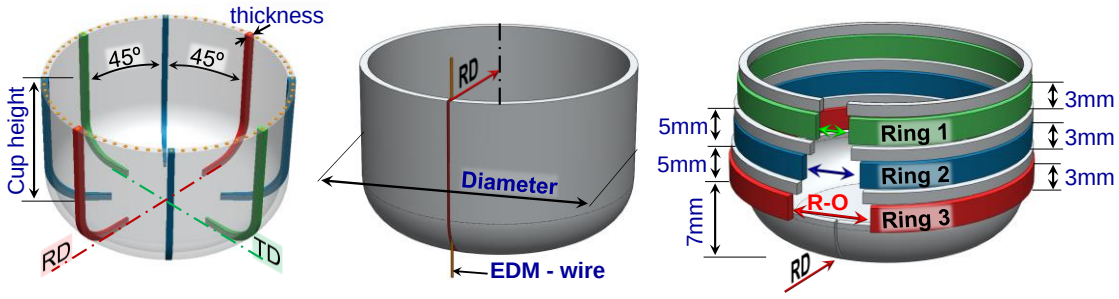

Figure 6 – Reference positions in the cylindrical cup for: a) measurements of thickness at each 45°, and of cup height at each 5° (the orange points) b) the vertical cut along RD with EDM-wire; and c) ring dimensions.

4.2 Results analysis and discussion

4.2.1 Punch force

The influence of temperature on the punch force evolution is presented in Figure 7 a) and b), for the EN AW 6016-T4 alloy and the EN AW 6061-T6 alloy, respectively. Two different phases are

distinguished: (i) the drawing and (ii) the ironing. The drawing phase occurs until a punch displacement of ≈ 21mm. During this phase, first, the punch force increases rapidly until a displacement of ≈11 mm, which corresponds to the instant that the die and the punch shoulder radii are completely formed in the part. Afterwards, it decreases until it reaches a local minimum at ≈19mm of punch displacement, which is related to the fact that the tool presents no blank-holder stopper (see Figure 5 a)). This minimum occurs just before the loss of contact between the blank and the blank-holder, since at this stage the blank-holder promotes the movement of the sheet into the die cavity and, consequently, reduces the punch force. The ironing phase can be associated with the increase of the punch force until attaining a local maximum (≈23mm of punch displacement), followed by a decrease until the end of the process. Ironing occurs since the gap between the punch and the die is not sufficiently large to allow the thicker material to flow. In fact, during the drawing phase, the material located in the flange area is submitted to a compression stress state in the circumferential direction (to reduce its diameter), which leads to an increase of the initial sheet thickness (see Table 1). Since, the material thickness becomes higher than the gap between the punch and the die (1.15 mm, see Figure 5 a)), the ironing of the cup wall will occur. Usually, the ironing is a process used to produce a more uniform wall thickness and increase the cup height [40]. This process is very complex since the cup wall is simultaneously stretched along the axial direction and squashed between the punch and the die in the through-thickness direction. Moreover, the ironing process imposes high contact forces, normal to the surface of the punch and the die, which can lead to the occurrence of galling, particularly for aluminum alloys in dry contact conditions [34, 41].

Globally, the punch force decreases with the temperature increase, correlating with the material softening behavior shown in Figure 1. The natural aging effect was evaluated only for the EN AW 6016-T4 alloy, by performing tests at 1 and 18 months of storage time. The results show an increase of the punch force due to the increase of the storage time, which is linked to the natural aging strengthening effect (see Figure 1 and Figure 3). However, this increase of the punch force due to natural aging becomes negligible as the temperature increases, which is in accordance with the results of the tensile tests (see Figure 1). Moreover, as described in Section 3.2.1, in the uniaxial tensile test at 200 °C the dissolution of natural aging clusters occurs for a test time of about 60 seconds. Therefore, since in the cylindrical cup test the heating phase takes 60 seconds,

a significant dissolution of natural aging clusters is expected. This may contribute to minimizing the variability in the punch force since the beginning of the drawing test. Lastly, for the same test conditions, the maximum punch force attained for the EN AW 6016-T4 alloy is always quite inferior to the one obtained for the EN AW 6061-T6 alloy, which confirms that the heating time selected avoids the occurrence of heat treatment changes.

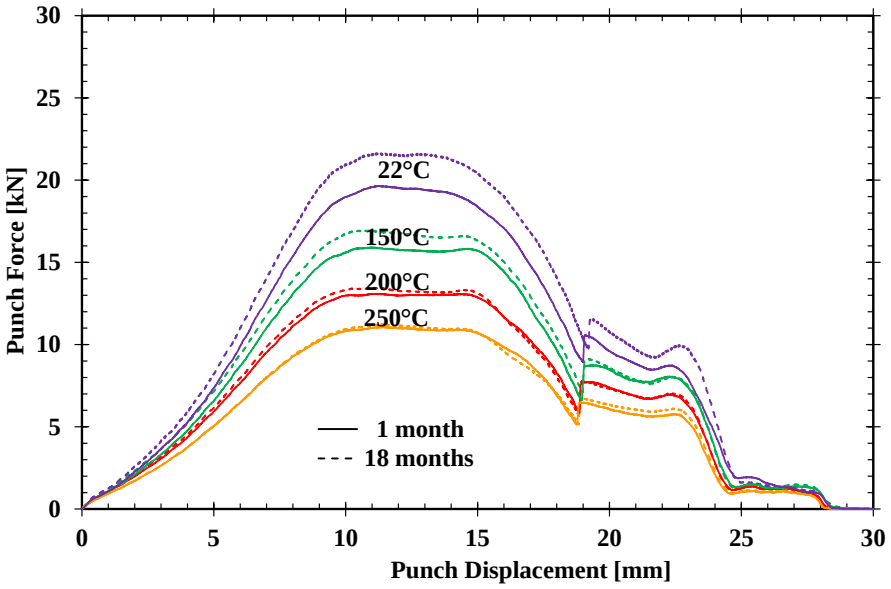

a) EN AW 6016-T4

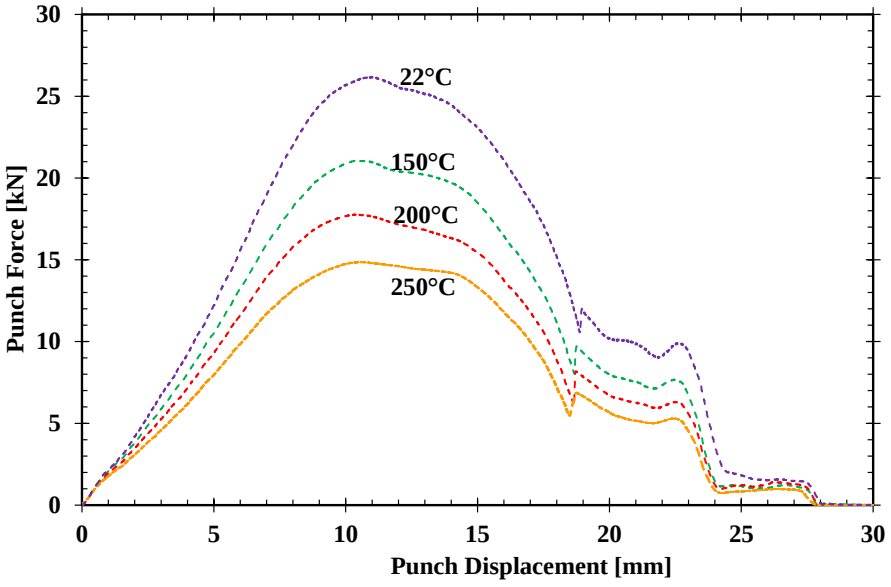

b) EN AW 6061-T6

Figure 7 – The influence of temperature and natural aging on the punch force evolution as a function of the punch displacement. The 1 month aged material is shown by the solid line and the 18 months by the dashed line.

The percentage variation of the maximum punch force in the drawing and the ironing stage can be determined considering the results at RT and at 18 months of storage time as reference. When the temperature increases from RT to 250 °C, for the EN AW 6016-T4 alloy, it is observed a drawing force reduction of ≈50% and an ironing force reduction of ≈40%; while for the EN AW 6061-T6 alloy, the drawing and the ironing phase present a similar percentage of punch force reduction of ≈40%. In fact, only for the EN AW 6016-T4 alloy the temperature increase seems to have a higher impact in the drawing stage than in the ironing one. Regarding the influence of natural aging on the punch force for the EN AW 6016-T4 alloy, at RT, 1 month aged specimens show a reduction of 8% in the drawing force and of 11% in the ironing force, as compared to the 18 months aged specimens.

4.2.2 Cylindrical Cup dimensions

The thickness evolution along the cup profile and the height are presented in Figure 8 a) and b), respectively. Since the thickness variations with the angle to RD are negligible, only the RD is presented. The cup height is shown in function of the angle to RD (from 0 to 90° to RD). Due to the volume conservation, the average cup height and the thickness distribution can be correlated. Globally, a higher cup height occurs associated with a lower average thickness value.

The thickness evolution along the cup profile is presented as a function of the curvilinear distance from the cup center up to its top, see Figure 8 a). Three distinct zones can be identified: cup bottom (0 up to 11 mm), punch radius (11 up to 20 mm) and vertical wall (20 mm up to end). The two critical points, where the thickness reaches local minima, are at the entrance to the punch radius section and the confluence of the punch radius with the cup wall [42]. After that, along the cup wall, the thickness increases and attains a constant final value, due to the ironing phase.

Globally, both alloys present a similar trend on the thickness evolution, which is not affected by the temperature or natural aging. The fact that the EN AW 6061-T6 alloy presents lower thickness values is linked with its lower average initial value of 0.98mm, while the EN AW 6061-T6 alloy has 1.05mm (see Table 1). Between RT and 200 °C, the thickness increases with the increase of temperature, stabilizing above 200 °C. The higher variation of the thickness with temperature occurs at the cup radius zone. According to Palumbo and Tricarico [43], this can be related with the strengthening effect produced by the cooled punch and with the material softening due to the

heated peripheral region that reduces the required punch load and, consequently, the stress and strains levels on the punch radius section. Additionally, the maximum force attained in the ironing phase is lower in the warm forming tests (see Figure 7), as compared to the RT one. The lower ironing force in warm forming tests is a consequence of the material thermal softening in the heated peripheral region, but it is also related with the thermal dilation of the die/punch and the consequent increase of the gap between them. In fact, considering that in warm forming conditions the temperature distribution in the die/punch is uniform and that there are no constraints to its displacement in the radial direction, the die/punch will expand. This increase of the gap with the increase of the test temperature is corroborated by the experimental results shown in Figure 8 a) and helps to explain why the warm formed cups always present a higher thickening.

The cup height distribution (or ear profile) is a consequence of the material anisotropic behavior. However, according to Yoon et al. [40], the ironing phase tends to increase the cup height while reducing the earing profile. The shape of the ear profile is similar for both alloys, with maxima at RD and 90° to RD, and minimum at 45° to RD and equivalent positions. This is the expected behavior for materials presenting $\Delta r > 0$ [44] (see Table 3). Temperature or natural aging does not affect the shape of the ear profile, confirming their subtle influence in the anisotropic behavior (see Section 3.2.3). In fact, a slight decrease of the cylindrical cup ears amplitude (the difference between the maximum and minimum height) was noticed with the increase of temperature. This is in agreement with the lower value of Δr reported for the tensile tests (see Table 3), as well as with other warm forming results [19, 35].

Concerning the effect of natural aging for the EN AW 6016-T4 alloy, globally the cups obtained from 18 months natural aged material are slightly thicker than the ones stored during 1 month, particularly for the tests performed at RT, consequently, its height profile is slightly lower. According to results obtained with finite element analysis, this seems to be mainly related to the increase in the flow stress induced by the natural aging [45]. However, this influence of natural aging in the cup thickness and height profile is reduced as the temperature increases, which correlates with the results of the tensile tests presented in Figure 1. Lastly, in agreement with the slight increase of the Δr value due to natural aging (see Table 3), the amplitude of the cup ears is higher for the 18 months aged material, when compared with 1 month.

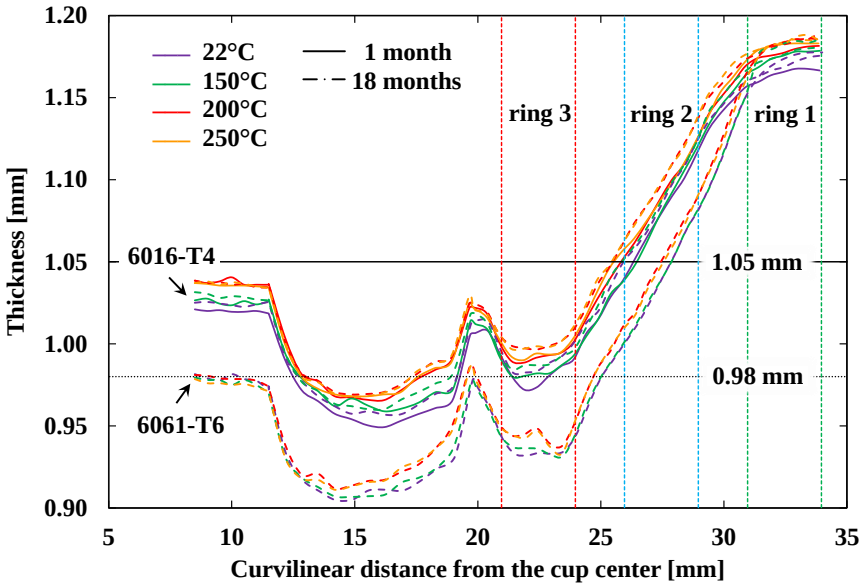

a) cup thickness

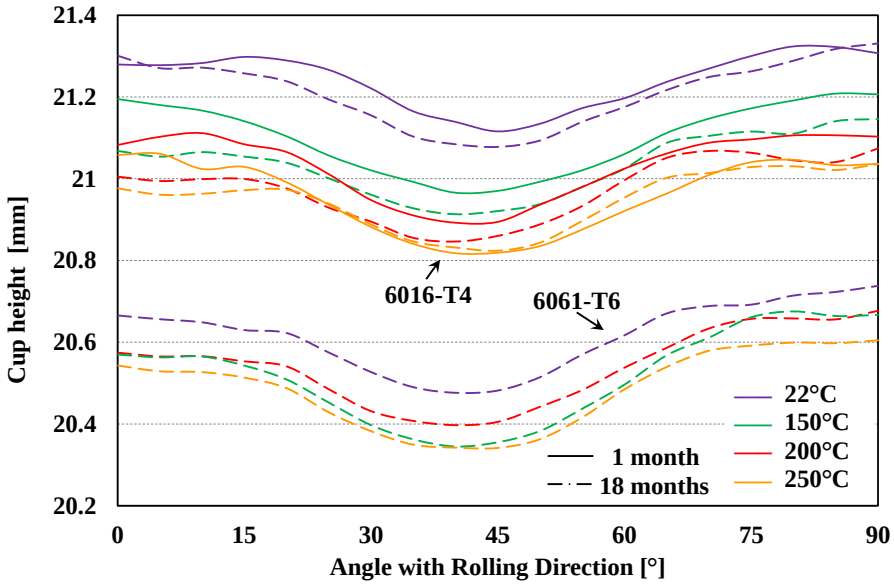

b) cup height

Figure 8 – The influence of temperature and natural aging on the cup dimensions. The 1 month aged material is shown by the solid line and the 18 months by the dashed-dot line.

4.2.3 Springback: the split ring test

The springback analysis based on the split ring test results is shown in Figure 9 a) and b) for the EN AW 6016-T4 and the EN AW 6061-T6 alloys, respectively. Concerning the influence of the axial position of the ring in the cup wall, it is observed that ring 3 (near to cup bottom) presents the highest opening value, while ring 1 (at the cup top) presents the lowest one, i.e. the ring

opening shows a decreasing value as the distance to the cup bottom increases. This trend occurs for both materials tested, at RT and warm forming; therefore, it cannot be assigned to the test temperature and the material behavior. It should be mentioned that different trends have been reported in the literature, such as the increase of the ring opening with the increase of the distance to the cup bottom [38], or the highest ring opening for the one located closer to the middle of the vertical wall [39]. The ring opening trend is dictated by the distribution of the residual stresses in the cup, which depends on the specific combination of the forming parameters selected to perform the deep drawing operation. This includes: the depth and diameter of the cup; the bending radii of the tools; the gap between the die and the punch; and the blank-holder force [46]. In the particular case under analysis, it is also influenced by the occurrence of the ironing stage, which contributes to the reduction of the through-thickness gradient of the circumferential stress component, leading to a smaller ring opening, as observed in [47, 48].

As shown in Figure 9, the opening of the rings 2 and 3 (Figure 6 c)) decreases linearly as the temperature increases, while ring 1 (at the cup top) presents an opening value relatively constant. In rings 2 and 3, the springback reduction is attributed to the material softening behavior promoted by the temperature increase [5, 49], which reduces the magnitude of the circumferential residual stresses in the deep drawn cups and, consequently, the ring opening. The fact that ring 1 presents a relatively constant springback value as the temperature increases seems to be connected to the ironing stage. Comparing the tests performed at RT with the ones at 250 °C, and considering as example ring 2 (at the middle): the EN AW 6016-T4 alloy with 18 months of storage time presents a springback decrease of 16%; while the EN AW 6061-T6 alloy presents a decrease of 26%. In this context, the results are coherent with the fact that the increase of temperature presents a stronger effect in the yield stress for the EN AW 6061-T6 alloy (see Figure 1). In fact, it is known that for the same Young modulus value, springback increases with the increase of the yield stress [4]. Therefore, for the same temperature, the EN AW 6016-T4 alloy always presents a lower springback value.

As shown in Figure 9 a) for the EN AW 6016-T4, the influence of natural aging in the springback variability is maximal at RT and decreases as the temperature increases, being negligible from 200 °C. The springback increases as the storage time increases, which is coherent with the variation reported for the yield stress as a function of natural aging (see Figure 3). These results

confirm the potential of warm forming to minimize the influence of natural aging on springback variability, while also reducing springback.

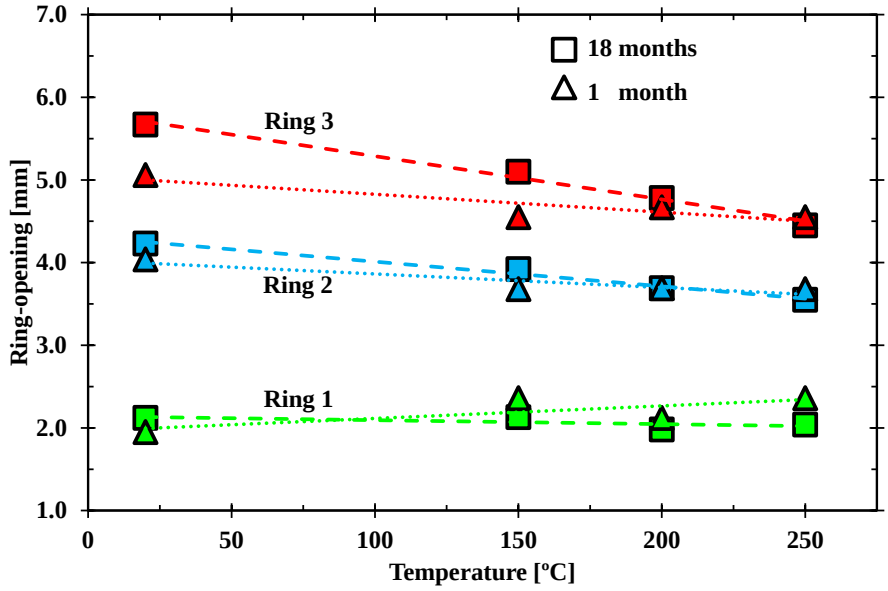

a) EN AW 6016-T4

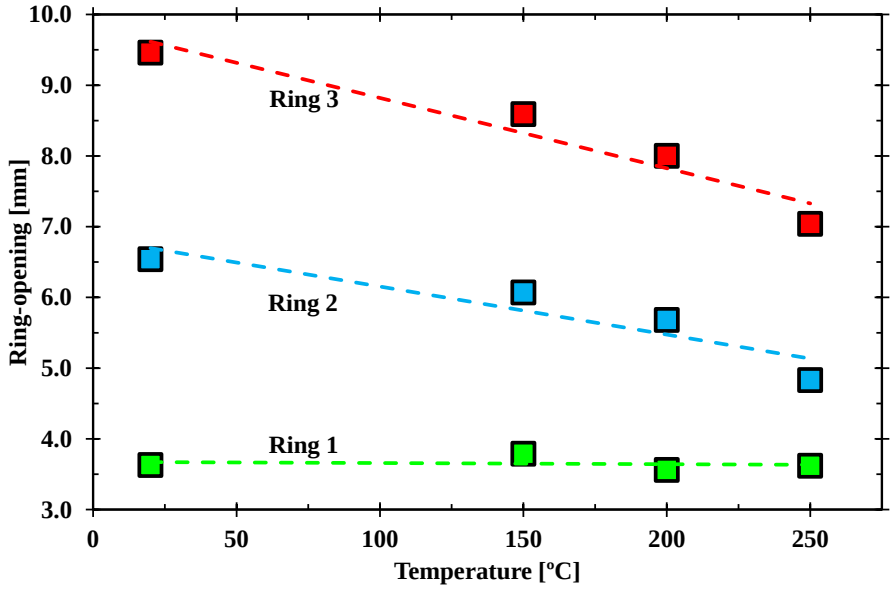

b) EN AW 6061-T6

Figure 9 – The influence of temperature and natural aging on the ring opening

5 Conclusions

Two Al-Mg-Si alloys (EN AW 6016-T4, EN AW 6061-T6) were analyzed using uniaxial tensile tests, cylindrical cup deep drawing tests and the split ring (springback) tests. The results show that:

- the mechanical behavior of the EN AW 6016-T4 alloy is strongly influenced by natural aging. At RT (from 1 to 18 months), the yield stress and tensile strength increase as the storage time increases, which leads to an increase of the maximum drawing forces (about 10%) and springback (about 10%).
- for both alloys, the temperature increase leads to a decrease of the yield stress and the work hardening rate. Compared to RT, warm forming reduces the drawing forces, indicating the presence of lower internal stress, which leads to lower springback values.
- the temperature increase leads to an increase of the post-uniform elongation, which is higher for the EN AW 6061-T6 alloy than for the EN AW 6016-T4 alloy, although it has a small influence in uniform elongation. This increase in ductility is advantageous to improve formability in sheet metal forming parts.
- concerning the orthotropic behavior, the trend does not change due to natural aging or temperature increase. However, the planar anisotropy coefficient slightly increases due to natural aging and decreases due to the temperature increase.
- the temperature increase reduces the influence of natural aging in the variations of yield stress and tensile strength. Thus, whatever the storage time, in warm forming between 200 and 250 °C, the drawing force required to produce the cylindrical cups is nearly the same, as well as the thickness evolution along the cup, and the springback. However, it should be mentioned that a short heating time is required to avoid relevant microstructural changes.

In summary, warm forming contributes to the increase of formability and springback reduction. Moreover, the results highlight the potential of warm forming in a temperature range from 200 to 250 °C as an effective solution to minimize the influence of natural aging in sheet metal forming parts variability. From an industrial point of view, warm forming can also be used to reduce the variability coming from different batches or different manufacturers.

Acknowledgements

The authors would like to acknowledge the funding that sponsored this research work: the national funds from the French Ministry of Higher Education and the Portuguese Foundation for Science and Technology (FCT) via the project P2020-PTDC/EMS-TEC/6400/2014 (POCI-01-0145-FEDER-016876) and by UE/FEDER funds through the program COMPETE 2020, under the project CENTRO-01-0145-FEDER-000014 (MATIS). The first author V. Simões is also grateful to the FCT for the PhD grant SFRH/BD/90669/2012. The authors are also grateful to Constellium (Estelle Muller) for supplying the material. Moreover, the authors acknowledge the technical staff of IRDL, for their help in some of the experimental procedures (Anthony Jégat and Hervé Bellegou).

Compliance with Ethical Standards

Funding: This study was funded by the French Ministry of Higher Education and the Portuguese Foundation for Science and Technology (FCT) via the project P2020-PTDC/EMS-TEC/6400/2014 (POCI-01-0145-FEDER-016876) and by UE/FEDER funds through the program COMPETE 2020, under the project CENTRO-01-0145-FEDER-000014 (MATIS). The first author V. Simões was also funded by the FCT for the PhD grant SFRH/BD/90669/2012.

Conflict of Interest: The authors declare that they have no conflict of interest.

References

1. Miller WS, Zhuang L, Bottema J, et al (2000) Recent development in aluminium alloys for the automotive industry. Mater Sci Eng A 280:37–49 . doi: 10.1016/S0921-5093(99)00653-X

2. Bolt PJ, Lamboo N, Rozier P (2001) Feasibility of warm drawing of aluminium products. J Mater Process Technol 115:118–121

3. Li D, Ghosh A (2003) Tensile deformation behavior of aluminum alloys at warm forming temperatures. Mater Sci Eng A 352:279–286 . doi: 10.1016/S0921-5093(02)00915-2

4. Moon YH, Kang SS, Cho JR, Kim TG (2003) Effect of tool temperature on the reduction of the springback of aluminum sheets. J Mater Process Technol 132:365–368 . doi: 10.1016/S0924-0136(02)00925-1

5. Grèze R, Manach PY, Laurent H, et al (2010) Influence of the temperature on residual stresses and springback effect in an Aluminium alloy. Int J Mech Sci 52:1094–1100 . doi: 10.1016/j.ijmecsci.2010.04.008

6. Hirsch J (2011) Aluminium in innovative light-weight car design. Mater Trans 52:818–824

7. Suri R, Otto K, Boothroyd G (1999) Variation Modeling for a Sheet Stretch Forming Manufacturing System. CIRP Ann - Manuf Technol 48:397–400 . doi: 10.1016/S0007-8506(07)63211-9

8. Zhong H, Rometsch P, Cao L, et al (2010) Tensile properties and work hardening behaviour of alloy 6016 in naturally aged and pre-aged conditions. In: Proceedings of the 12th International Conference on Aluminium Alloys. Japan Institute of Light Metals, Tokyo, Japan, pp 2203–2208

9. Leacock AG, Howe C, Brown D, et al (2013) Evolution of mechanical properties in a 7075 Al-alloy subject to natural ageing. Mater Des 49:160–167 . doi: 10.1016/j.matdes.2013.02.023

10. Marretta L, Lorenzo RD (2010) Influence of material properties variability on springback and thinning in sheet stamping processes: a stochastic analysis. Int J Adv Manuf Technol 51:117–134 . doi: 10.1007/s00170-010-2624-4

11. Prillhofer R, Rank G, Berneder J, et al (2014) Property Criteria for Automotive Al-Mg-Si Sheet Alloys. Materials 7:5047–5068 . doi: 10.3390/ma7075047

12. Ding L, Weng Y, Wu S, et al (2016) Influence of interrupted quenching and pre-aging on the bake hardening of Al–Mg–Si Alloy. Mater Sci Eng A 651:991–998 . doi: 10.1016/j.msea.2015.11.050

13. Yan Y (2014) Investigation of the negative and positive effect of natural aging on artificial aging response in Al-Mg-Si alloys. PhD-thesis, Technische Universität Berlin

14. Engler O, Schäfer C, Myhr OR (2015) Effect of natural ageing and pre-straining on strength and anisotropy in aluminium alloy AA 6016. Mater Sci Eng A 639:65–74 . doi: 10.1016/j.msea.2015.04.097

15. Werinos M, Antrekowitsch H, Ebner T, et al (2016) Hardening of Al–Mg–Si alloys: Effect of trace elements and prolonged natural aging. Mater Des 107:257–268 . doi: 10.1016/j.matdes.2016.06.014

16. Pogatscher S, Antrekowitsch H, Leitner H, et al (2011) Mechanisms controlling the artificial aging of Al–Mg–Si Alloys. Acta Mater 59:3352–3363 . doi: 10.1016/j.actamat.2011.02.010

17. Fan X, He Z, Zhou W, Yuan S (2016) Formability and strengthening mechanism of solution treated Al–Mg–Si alloy sheet under hot stamping conditions. J Mater Process Technol 228:179–185 . doi: 10.1016/j.jmatprotec.2015.10.016

18. Kumar M, Poletti C, Degischer HP (2013) Precipitation kinetics in warm forming of AW-7020 alloy. Mater Sci Eng A 561:362–370 . doi: 10.1016/j.msea.2012.10.031

19. Ghosh M, Miroux A, Werkhoven RJ, et al (2014) Warm deep-drawing and post drawing analysis of two Al–Mg–Si alloys. J Mater Process Technol 214:756–766 . doi: 10.1016/j.jmatprotec.2013.10.020

20. AMAG (2012) AluReport 03/2012 - 7xxx-high strength aluminum sheets for lightweight automotive applications. 6–9

21. Banhart J, Chang CST, Liang Z, et al (2010) Natural Aging in Al-Mg-Si Alloys - A Process of Unexpected Complexity. Adv Eng Mater 12:559–571 . doi: 10.1002/adem.201000041

22. ISO 6892-1:2009 (2009) Metallic materials - Tensile testing - Part 1: Method of test at room temperature. International Organization for Standardization, Geneva, Switzerland

23. Kurukuri S (2010) Simulation of thermally assisted forming of aluminium sheet. PhD-thesis, University of Twente

24. Kaufman JG (2008) Properties of Aluminum Alloys: Fatigue Data and Effects of Temperature, Product Form, and Processing. ASM International, Materials Park, Ohio : Washington, D.C

25. The Aluminum Association (2015) International Alloy Designations and Chemical Composition Limits for Wrought Aluminum and Wrought Aluminum Alloys

26. Coër J, Bernard C, Laurent H, et al (2011) The Effect of Temperature on Anisotropy Properties of an Aluminium Alloy. Exp Mech 51:1185–1195 . doi: 10.1007/s11340-010-9415-6

27. Mahabunphachai S, Koç M (2010) Investigations on forming of aluminum 5052 and 6061 sheet alloys at warm temperatures. Mater Des 1980-2015 31:2422–2434 . doi: 10.1016/j.matdes.2009.11.053

28. Ayres RA (1977) Enhanced ductility in an aluminum-4 Pct magnesium alloy at elevated temperature. Metall Trans A 8:487–492 . doi: 10.1007/BF02661760

29. Shehata F, Painter MJ, Pearce R (1978) Warm forming of aluminium/magnesium alloy sheet. J Mech Work Technol 2:279–290 . doi: 10.1016/0378-3804(78)90023-2

30. Esmaeili S, Lloyd DJ (2004) Effect of composition on clustering reactions in AlMgSi(Cu) alloys. Scr Mater 50:155–158 . doi: 10.1016/j.scriptamat.2003.08.030

31. Hirth SM, Marshall GJ, Court SA, Lloyd DJ (2001) Effects of Si on the aging behaviour and formability of aluminium alloys based on AA6016. Mater Sci Eng A 319–321:452–456 . doi: 10.1016/S0921-5093(01)00969-8

32. Ding L, Jia Z, Zhang Z, et al (2015) The natural aging and precipitation hardening behaviour of Al-Mg-Si-Cu alloys with different Mg/Si ratios and Cu additions. Mater Sci Eng A 627:119–126 . doi: 10.1016/j.msea.2014.12.086

33. Banhart J, Lay MDH, Chang CST, Hill AJ (2011) Kinetics of natural aging in Al-Mg-Si alloys studied by positron annihilation lifetime spectroscopy. Phys Rev B 83:14101 . doi: 10.1103/PhysRevB.83.014101

34. Coër J, Laurent H, Oliveira MC, et al (2017) Detailed experimental and numerical analysis of a cylindrical cup deep drawing: Pros and cons of using solid-shell elements. Int J Mater Form 1–17 . doi: 10.1007/s12289-017-1357-4

35. Laurent H, Coër J, Manach PY, et al (2015) Experimental and numerical studies on the warm deep drawing of an Al–Mg alloy. Int J Mech Sci 93:59–72 . doi: 10.1016/j.ijmecsci.2015.01.009

36. Jelt Grease 5411 aerosol 95cSt. http://fr.rs-online.com/web/p/graisses/4612124/. Accessed 25 Nov 2015

37. ASTM E2492-07(2012) (2012) Standard Test Method for Evaluating Springback of Sheet Metal Using the Demeri Split Ring Test. ASTM Int 03.01: . doi: 10.1520/E2492-07R12

38. Gnaeupel-Herold T, Foecke T, Prask HJ, Fields RJ (2005) An investigation of springback stresses in AISI-1010 deep drawn cups. Mater Sci Eng A 399:26–32 . doi: 10.1016/j.msea.2005.02.017

39. Xia ZC, Miller CE, Ren F (2004) Springback Behavior of AA6111-T4 with Split-Ring Test. In: AIP Conference Proceedings. AIP Publishing, pp 934–939

40. Yoon JW, Dick RE, Barlat F (2011) A new analytical theory for earing generated from anisotropic plasticity. Int J Plast 27:1165–1184 . doi: 10.1016/j.ijplas.2011.01.002

41. Simões VM, Coër J, Laurent H, et al (2013) Sensitivity Analysis of Process Parameters in the Drawing and Ironing Processes. Key Eng Mater 554–557:2256–2265 . doi: 10.4028/www.scientific.net/KEM.554-557.2256

42. Colgan M, Monaghan J (2003) Deep drawing process: analysis and experiment. J Mater Process Technol 132:35–41 . doi: 10.1016/S0924-0136(02)00253-4

43. Palumbo G, Tricarico L (2007) Numerical and experimental investigations on the Warm Deep Drawing process of circular aluminum alloy specimens. J Mater Process Technol 184:115–123 . doi: 10.1016/j.jmatprotec.2006.11.024

44. Hu P, Liu YQ, Wang JC (2001) Numerical study of the flange earring of deep-drawing sheets with stronger anisotropy. Int J Mech Sci 43:279–296 . doi: 10.1016/S0020-7403(99)00119-8

45. Simões VM, Laurent H, Oliveira MC, Menezes LF (2016) Natural aging effect on the forming behavior of a cylindrical cup with an Al-Mg-Si alloy. AIP Conf Proc 1769:200021 . doi: 10.1063/1.4963639

46. Xiao L-H, Yuan D-H, Xiang J-Z, et al (2016) Residual stress in the cylindrical drawing cup of SUS304 stainless steel evaluated by split-ring test. Acta Mech Sin 32:125–134 . doi: 10.1007/s10409-015-0516-4

47. Ragab MS, Orban HZ (2000) Effect of ironing on the residual stresses in deep drawn cups. J Mater Process Technol 99:54–61 . doi: 10.1016/S0924-0136(99)00360-X

48. Simões VM, Oliveira MC, Neto DM, et al (2017) Numerical study of springback using the split-ring test: influence of the clearance between the die and the punch. Int J Mater Form 1–13 . doi: 10.1007/s12289-017-1351-x

49. Laurent H, Grèze R, Manach PY, Thuillier S (2009) Influence of constitutive model in springback prediction using the split-ring test. Int J Mech Sci 51:233–245 . doi: 10.1016/j.ijmecsci.2008.12.010